3D magnetization vector inversion for SQUID-based full tensor magnetic gradiometry

Michael S. Zhdanov, Martin Čuma, University of Utah and TechnoImaging, Glenn A. Wilson, TechnoImaging, and Louis Polomé, Spectrem Air*

Summary

Following recent advances in superconducting quantum interference devices (SQUIDs), airborne full tensor magnetic gradiometry (FTMG) is emerging as a practical geophysical exploration method that is intended to recover information about remanent magnetization. In this paper, we introduce 3D regularized inversion of FTMG data that recovers the total magnetization vector in each cell of the 3D earth model. If a priori information about the susceptibility or remanent magnetization is available, the 3D inversion can be constrained to recover the remanent magnetization vector. If a priori information is not available, it is possible to recover attributes such as the amplitude, components, and angle of the magnetization vector relative to the inducing field. We present a case study for data acquired over a dike swarm in South Africa that compares our 3D FTMG inversion for magnetization with a 3D total magnetic intensity (TMI) inversion for a positively-constrained susceptibility distribution. Given the significant remanent magnetization present, the 3D FTMG inversion for magnetization recovers results that are most consistent with the known geology.

Introduction

As discussed by Schmidt and Clark (2006), the direct measurements of magnetic gradients are advantageous for geophysical exploration for a number of reasons. First, magnetic gradients are relatively insensitive to instrument orientation since magnetic gradients arise largely from localized sources and not the Earth's background field or regional trends. Second, magnetic gradient data obviates the need for base stations and diurnal corrections. Third, magnetic tensor data contain directional sensitivity which is advantageous for the interpretation of under-sampled surveys. Fourth, information about remanent magnetization can be recovered from magnetic gradient data. This latter point is critical for exploration, as the Earth's magnetic field is non-stationary over geological time, meaning that the direction of magnetization in a rock differs from the direction of today's magnetic field. This is particularly relevant for historically emplaced magnetic structures such as kimberlites, dykes, iron-rich ultramafic pegmatitoids (IRUP), platinum group element (PGE) reefs, and banded iron formations (BIF) (Rompel, 2009).

The most appropriate sensors for full tensor magnetic gradiometry (FTMG) are superconducting quantum interference devices (SQUIDs) which detect changes of flux threading a superconducting loop. SQUIDs are therefore variometers rather than magnetometers, but they are vector sensors since only changes perpendicular to the loop are detected (Foley and Leslie, 1998; Foley et al., 1999; Lee et al., 2001). SQUID-based magnetic gradiometers were originally developed for real-time magnetic anomaly detection and surveillance for unexploded ordinance and naval warfare. Recently, SQUID-based magnetic gradiometers have also been developed for mineral exploration (e.g., Schmidt et al., 2004; Stolz et al., 2006). For real-time anomaly detection and surveillance, magnetic gradients have usually been interpreted by some form of direct source inversion (e.g., Wynn et al., 1975). While such methods can provide source location information, it is not immediately obvious how that information could be related to the magnetic properties of 3D earth models as required for geophysical exploration. For this, methods of eigenvector analysis have been developed (e.g., Holstein et al., 2011). Yet, there remains a need for a generalized 3D inversion which discretizes the 3D earth model into a grid of N_m cells populated with magnetic properties.

Magnetization vector-based 3D modeling and inversion

Most 3D magnetic inversion methods in use today are based on TMI or total field gradient data that recover a 3D magnetic susceptibility model, and assume that there is no remanent magnetization, that self-demagnetization effects are negligible, and that the magnetic susceptibility is isotropic (e.g., Li and Oldenburg, 1996, 2003; Portniaguine and Zhdanov, 2002; Zhdanov et al., 2012; Čuma et al., 2012). This implies that the magnetization is linearly proportional to the inducing magnetic field. Modeling with this approach manifests itself as the linear operator equation:

$$\mathbf{H} = \mathbf{A}_\chi \boldsymbol{\chi}, \tag{1}$$

where $\mathbf{H}$ is the N_d length vector of observed data, $\boldsymbol{\chi}$ is the N_m length vector of susceptibilities, and $\mathbf{A}_\chi$ is an $N_m \times N_d$ linear operator of Green's functions. Both $\mathbf{H}$ and $\mathbf{A}_\chi$ may be partitioned for joint modeling and inversion of multiple component magnetic data. To include both induced and remanent magnetization, we need to model on the magnetization vector rather than the scalar susceptibility (e.g., Lelièvre and Oldenburg, 2009; Ellis et al., 2012). This modifies equation (1) to the linear operator equation:

$$\mathbf{H} = \mathbf{A}_\mathrm{M} \mathbf{M}, \tag{2}$$

DOI http://dx.doi.org/10.1190/segam2012-0740.1

where $\mathbf{M}$ is the $3N_m$ length vector of magnetization vector components, and $\mathbf{A}_{\mathrm{M}}$ is now a $3N_m \times N_d$ matrix of linear forward modeling operator. Again, both $\mathbf{H}$ and $\mathbf{A}_{\mathrm{M}}$ may be partitioned for joint modelling and inversion of multiple component magnetic data. For inversion, we utilize the same regularized reweighted conjugate gradient (RRCG) method with focusing regularization as described by Zhdanov (2002) and implemented by Čuma et al. (2012). Given the relatively localized sensitivity of an FTMG system, we have also implemented a moving sensitivity domain. The method described enables explicit inversion of the magnetization direction and amplitude. We note that tripling the number of model parameters increases non-uniqueness. However, various constraints can be applied. For example, the directions of the magnetization can be set identical to the inducing field, and magnetization equivalent to the susceptibility will be recovered. Also, a priori knowledge of the amplitude and/or direction of remanent magnetization can be introduced. In our work, we have generalized the method for both vector and tensor magnetic data. For example, the elements of equation (2) for the magnetic tensor components can be written as:

$$H_{\alpha\beta}(\mathbf{r}') = -3H_0 \sum_{k=1}^{N_m} \frac{\Delta x \Delta y \Delta z}{|\mathbf{r}-\mathbf{r}'|^5} \sum_{\gamma=x,y,z} G^{\gamma}_{\alpha\beta k} M_{\gamma k}, \quad (3)$$

where, $\alpha, \beta = x, y, z$, H_0 is the amplitude of the inducing field, G is an appropriate Green's function, and $M_{\gamma k}$ are the components of the magnetization vector for the k^{th} cell:

$$\mathbf{M}_k = \left[M_{xk}, M_{yk}, M_{zk}\right]^{\mathrm{T}}. \quad (4)$$

Model study

We present an FTMG model study for a SW-NE trending dike that extends from the surface to 300 m depth. The inducing field is representative of a location in South Africa, with an inclination of -65$^{\mathrm{o}}$ and declination of -20$^{\mathrm{o}}$. The dike has remanent magnetization five times larger than the induced field, and is directed with an inclination of 30$^{\mathrm{o}}$ and declination of 45$^{\mathrm{o}}$ (Figure 1). We simulated FTMG data. As this model study was to investigate the mechanics of magnetization vector inversion, we did not contaminate the synthetic FTMG data with noise. We ran our inversion for 50 iterations with a minimum norm stabilizer, resulting in a final misfit less than 1%. An example of the result obtained from our inversion is shown in Figure 2. For comparison, we also calculated the TMI data and inverted that with no positivity enforced upon the susceptibility (Figure 3). As expected, there was poor convergence, and the resolved model has a large negative susceptibility area, indicating reverse direction of the magnetization. Inverting for susceptibility with positivity enforcement led to no convergence.

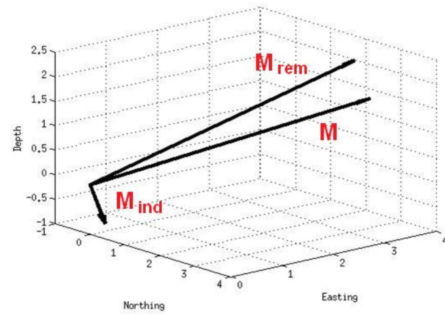

Figure 1. *Example of the magnetic properties of the dike, with the remanent magnetization five times larger than the induced magnetization.*

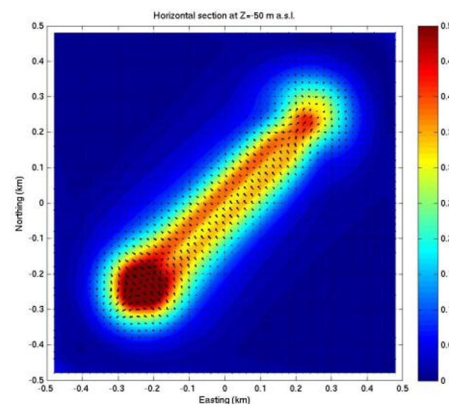

Figure 2. *Magnetization vector amplitude at 50 m depth as recovered from 3D magnetization vector inversion of synthetic FTMG data.*

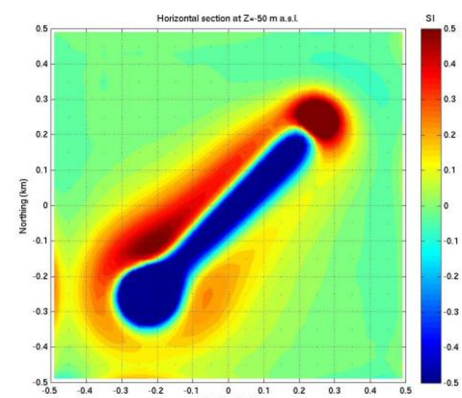

Figure 3. *Susceptibility at 50 m depth as recovered from 3D inversion of synthetic TMI data).*

Case study – South Africa

Spectrem Air operates a commercial airborne SQUID-based FTMG system developed by Anglo American and De Beers in collaboration with the Institute for Photonic Technologies (IPHT) in Jena, Germany (Figure 4). In the following case study, we compare results for a 3D susceptibility inversion of TMI data, and the 3D magnetization inversion of FTMG data (Figure 5). Both surveys were acquired over a known dyke swarm in a platinum reef in South Africa. The TMI data are characterized by a significant (10,000 nT) TMI low. The 7 km x 7 km x 1.2 km earth model was discretized into 25 m^3 cells. While the 3D susceptibility inversion will attempt to converge and fit the data (final misfit ~29%), the physical constraint of positive susceptibility leads to a geologically unreasonable susceptibility model (Figure 6). The 3D magnetization vector inversion is able to fit all magnetic tensors with a geologically reasonable magnetization model that corresponds to the known dyke locations (final misfit ~8%) (Figure 7). As this data is from an active exploration project, the geology cannot be presented.

Figure 4. *Spectrem Air's airborne SQUID-based FTMG system (upper panel) and in operation (lower panel).*

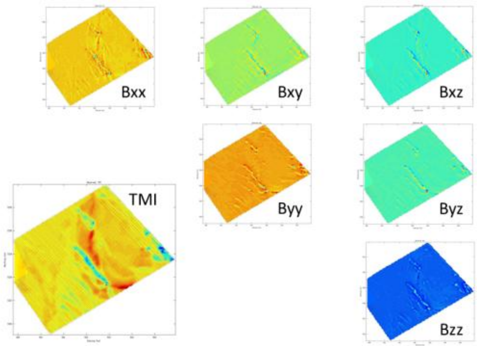

Figure 5. *TMI and FTMG data acquired over a dike swarm in South Africa.*

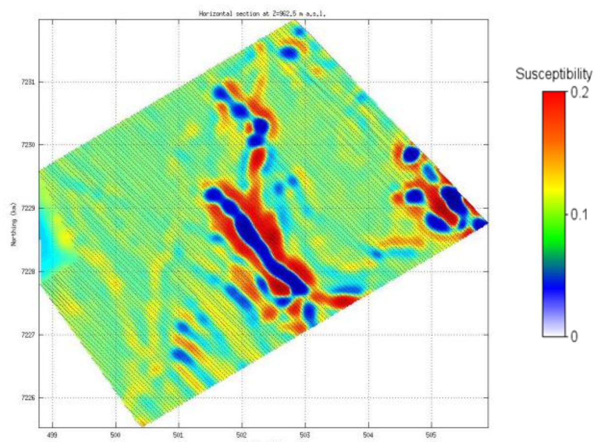

Figure 6. *Horizontal cross section of the positivity-enforced 3D susceptibility model at 50 m depth as recovered from 3D TMI inversion. Note that the inversion fails to recover any susceptibility in the actual location of the dike. Scales have been redacted for confidentiality.*

There is a very good consistency between the results of our synthetic model study, and the inversions of both FTMG and TMI data from the dike swarm in South Africa. This suggests that in practical exploration, it is advantageous to only use magnetization vector inversions, rather than use susceptibility inversions where remanent magnetization may distort the recovered models.

DOI http://dx.doi.org/10.1190/segam2012-0740.1

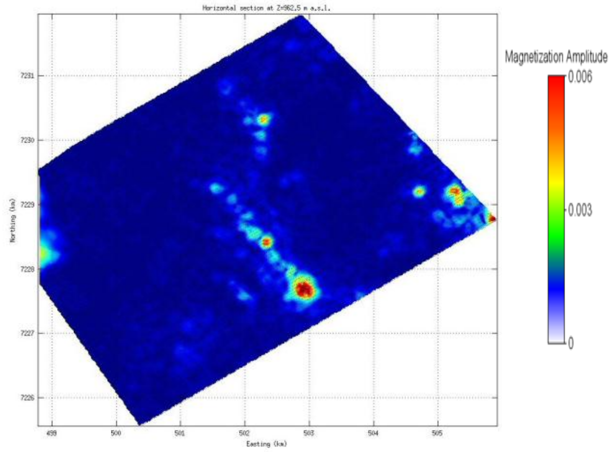

Figure 7. *Horizontal cross section of the 3D magnetization amplitude model at 50 m depth as recovered from 3D FTMG inversion. Scales have been redacted for confidentiality.*

We note that a similar conclusion was reached by Ellis et al. (2012). Similarly to their observations, many TMI data that we have processed converge poorly with susceptibility positively enforced and trend to negative susceptibility anomalies when no positivity enforcement is in place. The negative susceptibility anomalies are indicative of reverse direction of magnetization vector as compared to the Earth's inducing field.

Conclusions

FTMG data has higher spatial sensitivity and contains more information about magnetic bodies than scalar TMI data. To extract this information, we have developed 3D regularized inversion for FTMG data that can recover attributes of the magnetization. We have demonstrated this with a case study for a dyke swarm in South Africa that compares our 3D FTMG inversion for magnetization with a 3D total magnetic intensity (TMI) inversion for a positively-constrained susceptibility distribution. Given the significant remanent magnetization present, the 3D FTMG inversion for magnetization recovers results that are consistent with the known geology, whereas the 3D TMI inversion for susceptibility assuming induction only fails to recover a geologically realistic model.

Acknowledgements

The authors acknowledge TechnoImaging, Spectrem Air, and AngloAmerican Platinum for support of this research and permission to publish. Andy Rompel, Jaco Smit, Shawn Letts, and Anre Vorster are thanked for their contributions. Čuma and Zhdanov acknowledge support of the University of Utah's Consortium for Electromagnetic Modeling and Inversion (CEMI) and Center for High Performance Computing (CHPC).

DOI http://dx.doi.org/10.1190/segam2012-0740.1

http://dx.doi.org/10.1190/segam2012-0740.1

EDITED REFERENCES

Note: This reference list is a copy-edited version of the reference list submitted by the author. Reference lists for the 2012 SEG Technical Program Expanded Abstracts have been copy edited so that references provided with the online metadata for each paper will achieve a high degree of linking to cited sources that appear on the Web.

REFERENCES

Cuma M., G. A. Wilson, and M. S. Zhdanov, 2012, Large-scale 3D inversion of potential field data: Geophysical Prospecting, **60**, doi: 10.1111/j.1365-2478.2011.01052.x.

Ellis, R. G., B. de Wet, and I. McLeod, 2012, Inversion of magnetic data from remanent and induced sources: Presented at 22nd Geophysical Conference and Exhibition, ASEG.

Foley, C. P., and K. E. Leslie, 1998, Potential use of high-TC SQUIDs for airborne electromagnetics: Exploration Geophysics, **29**, 30–34.

Foley, C. P., K. E. Leslie, R. Binks, C. Lewis, W. Murray, G. J. Sloggett, S. Lam, B. Sankrithyan, N. Savvides, A. Katzaros, K. H. Muller, E. E. Mitchell, J. Pollock, J. Lee, D. L. Dart, R. R. Barrow, M. Asten, A. Maddever, G. Panjkovic, M. Downey, C. Hoffman, and R. Turner, 1999, Field trials using HTS SQUID magnetometers for ground-based and airborne geophysical applications: IEEE Transactions on Applied Superconductivity, **9**, 3786–3792.

Holstein H., D. Fitzgerald, C. P. Willis, and C. Foss, 2011, Magnetic gradient tensor Eigen-analysis for dyke location: Presented at 73rd Annual International Conference and Exhibition, EAGE.

Lee, J. B., R. J. Turner, M. A. Downey, A. Maddever, D. L. Dart, C. P. Foley, R. Binks, C. Lewis, W. Murray, G. Panjkovic, and M. Asten, 2001, Experience with SQUID magnetometers in airborne TEM surveying: Exploration Geophysics, **32**, 9–13.

Lelièvre, P. G., and D. W. Oldenburg, 2009, A 3D total magnetization inversion applicable when significant, complicated remanence is present: Geophysics, **74**, no. 3, L21–L30.

Li, Y., and D. W. Oldenburg, 1996, 3D inversion of magnetic data: Geophysics, **61**, 394–408.

Li, Y., and D. W. Oldenburg, 2003, Fast inversion of large-scale magnetic data using wavelet transforms and a logarithmic barrier method: Geophysical Journal International, **152**, 251–265.

Portniaguine, O., and M. S. Zhdanov, 2002, 3D magnetic inversion with data compression and image focusing: Geophysics, **67**, 1532–1541.

Rompel, A. K. K., 2009, Geologic applications of FTMG: Presented at 11th Biennial Technical Meeting and Exhibition, SAGA.

Schmidt, P. W., and D. A. Clark, 2006, The magnetic gradient tensor — Its properties and uses in source characterization: The Leading Edge, **25**, 75–78.

Schmidt, P., D. Clark, K. E. Leslie, M. Bick, D. L. Tilbrook, and C. P. Foley, 2004, GETMAG — A SQUID magnetic tensor gradiometer for mineral and oil exploration: Exploration Geophysics, **35**, 297–305.

Stolz, R., V. Zakosarenko, M. Schulz, A. Chwala, L. Fritzsch, H. G. Meyer, and E. O. Kostlin, 2006, Magnetic full-tensor SQUID gradiometer system for geophysical applications: The Leading Edge, **25**, 178–180.

Wynn, W. M., C. P. Frahm, P. J. Carroll, R. H. Clark, J. Wellhoner, and M. J. Wynn, 1975, Advanced superconducting gradiometer/magnetometer arrays and a novel signal processing technique: IEEE Transactions on Magnetics, **11**, 701–707.

Zhdanov, M. S., 2002, Geophysical inverse theory and regularization problems: Elsevier.

Zhdanov, M. S., X. Liu, G. A. Wilson, and L. Wan, 2012, 3D migration for rapid imaging of total-magnetic-intensity data: Geophysics, **77**, no. 2, J1–J5.